

Meson Correlators at Finite Temperature

Varun Sheel*, Hiranmaya Mishra and Jitendra C. Parikh

Theory Division, Physical Research Laboratory, Navrangpura, Ahmedabad 380 009, India

Abstract

We evaluate equal time point to point spatial correlation functions of mesonic currents at finite temperature. For this purpose we consider the QCD vacuum structure in terms of quark antiquark condensates and their fluctuations in terms of an irreducible four point structure of the vacuum. The temperature dependence of quark condensates is modeled using chiral perturbation theory for low temperatures and lattice QCD simulations near the critical temperature. We first consider the propagation of quarks in a condensate medium at finite temperature. We then determine the correlation functions in a hot medium. Parameters such as mass, coupling constant and threshold energy are deduced from the finite temperature correlators. We find that all of them decrease close to the critical temperature.

PACS number(s): 12.38.Gc

Typeset using REVTeX

*Electronic address: varun@prl.ernet.in

I. INTRODUCTION

The structure of vacuum in Quantum Chromodynamics (QCD) is one of the most interesting question in strong interaction physics [1]. The evidence for quark and gluon condensates in vacuum is a reflection of its complex nature [2]. Determination of correlation functions [3,4] of hadronic currents in such a vacuum state provides rich information regarding interquark interaction as a function of their spatial separation as well as on hadron spectroscopy. These are some of the nonperturbative feature of QCD and are of great value in understanding the ground state structure of the theory of strong interactions [3,4].

We have studied mesonic and baryonic current correlators at zero temperature with a non-trivial structure for the ground state with quark antiquark condensates [5,6]. It was shown that the square of the quark propagator does not reproduce the correlation function for the pion deduced from phenomenology. In order to match the data it was necessary to introduce an irreducible four point structure for the quarks in the vacuum. This may be looked upon as an effective way of incorporating gluon condensate contribution to the correlator.

As is well known [7] the QCD vacuum state changes with temperature. Lattice monte carlo simulations suggest that chiral symmetry is restored around 150 MeV. In view of this the present note is aimed at looking at the behaviour of the meson correlation functions at finite temperature. This is of great interest in the context of behaviour of hadrons around the chiral phase transition associated with quark gluon plasma [8,9]. It may be noted that there is little phenomenological information in this regime but there are several theoretical studies [10] essentially using sum rule methods. The main objective here is to employ a different nonperturbative approach developed by us [11]. This has been sucessful at zero temperature, and, its extension to finite temperature is therefore of interest. In particular, we will obtain temperature dependence of masses, coupling constants and threshold energies for the pion and rho mesons.

We organise the paper as follows. In section II we discuss the quark condensate at finite

temperature to fix the parameter appearing in the ansatz of the ground state of QCD. We then discuss in section III the quark propagation in the thermal vacuum. In section IV we calculate meson correlation functions at finite temperature. Finally we discuss the results in section V.

II. QUARK CONDENSATE AT FINITE TEMPERATURE

To calculate the correlators at finite temperature we need the expression for the equal time propagator for the interacting quark field operators. We have developed earlier [5] a vacuum structure in terms of quark antiquark condensates with a condensate function $h(k)$. The equal time propagator could then be calculated in terms of the condensate function [6]. One can generalise this to finite temperature using the method of thermofield dynamics. Here the thermal average is obtained as an expectation value of the operator over the thermal vacuum [12]. This leads to

$$\begin{aligned}\langle \psi_\alpha^i(\vec{x}) \psi_\beta^{j\dagger}(\vec{0}) \rangle_T &= \frac{\delta^{ij}}{(2\pi)^3} \int e^{i\vec{k}\cdot\vec{x}} \Lambda_{+\alpha\beta}(\vec{k}, T) d\vec{k} \\ \langle \psi_\alpha^{i\dagger}(\vec{x}) \psi_\beta^j(\vec{0}) \rangle_T &= \frac{\delta^{ij}}{(2\pi)^3} \int e^{-i\vec{k}\cdot\vec{x}} \Lambda_{-\beta\alpha}(\vec{k}, T) d\vec{k}\end{aligned}\quad (1)$$

The thermal vacuum is obtained from the zero temperature vacuum by a thermal Bogoliubov transformation in an extended Hilbert space involving extra field operators (thermal doubling of operators) [12]. The functions Λ_\pm (Eq. 1) for the case of two flavour massless quarks, are given as (with $k = |\vec{k}|$),

$$\Lambda_\pm(\vec{k}, T) = \frac{1}{2} \left[1 \pm \cos 2\theta(\gamma^0 \sin 2h(k) + \vec{\alpha} \cdot \hat{k} \cos 2h(k)) \right]. \quad (2)$$

In the above $h(k)$ is the condensate function [5,6,11] corresponding to the Bogoliubov transformation to include a condensate structure in the vacuum. The function θ is associated with the thermal Bogoliubov transformation and is related to the distribution function as [12]

$$\sin^2 \theta(k) = \frac{1}{\exp[\beta\epsilon(k)] + 1}, \quad (3)$$

β being the inverse temperature. Further $\epsilon(k)$ is the single particle energy given as $\epsilon(k) = \sqrt{k^2 + m(k)^2}$. In the presence of condensate the dynamical mass is given as $m(k) = m + k \tan 2h(k)$, m being a possible current quark mass [5].

We had earlier taken a gaussian ansatz for the condensate function $\sin 2h(k) = e^{-R^2 k^2/2}$. In order to determine the parameter R , we had taken a value of R consistent with hadronic correlator phenomenology. We choose a similar structure for the condensate function at finite temperature namely $\sin 2h(k) = e^{-R(T)^2 k^2/2}$ with $R(T)$ now being temperature dependent.

In order to determine $R(T)$ or equivalently the ratio $S(T) = R(T=0)/R(T)$, we first evaluate our expression of the order parameter (the condensate value) at finite temperature. In terms of the dimensionless variable $\eta = Rk$, this is given as

$$\frac{\langle \bar{q}q \rangle_T}{\langle \bar{q}q \rangle_{T=0}} = S(T)^3 \left[1 - 2\sqrt{\frac{2}{\pi}} \int e^{-\eta^2/2} \sin^2(z, \eta) \eta^2 d\eta \right], \quad (4)$$

where $\sin^2 \theta(z, \eta) = \frac{1}{e^{z\epsilon(\eta)} + 1}$, with $z = \beta/R(T)$ and $\epsilon(\eta) = \eta/\cos 2h(\eta)$.

We can obtain $S(T) = R(T=0)/R(T)$ if we know the temperature dependence of the order parameter on the left hand side of Eq.(4). As there are no phenomenological inputs for this, we shall consider the results from chiral perturbation theory (CHPT) which is expected to be valid at least for small temperatures. For higher temperatures near the critical temperature, lattice simulations seem to yield the universal behaviour [7] with a large correlation length associated with a second order phase transition for two flavor massless QCD. We shall use such a critical behaviour to consider the temperature dependence of the order parameter near the critical temperature.

We quote here the results of CHPT obtained by Gerber and Leutwyler [13]. The condensate ratio at temperatures small compared to the pion mass is given as

$$\frac{\langle \bar{q}q \rangle_T}{\langle \bar{q}q \rangle_{T=0}} = 1 + \frac{c}{F^2} \left[\frac{3}{2} T^4 h'_0 + 4\pi T^4 (a' h_1^2 + 2a h_1 h'_1) + \pi T^8 (h' b_{eff} + b'_{eff} h) \right]. \quad (5)$$

where the functions h are defined as

$$\begin{aligned} h_0 &= H^4(\mu)/(3\pi^2) & h'_0 &= -H^2(\mu)/(2\pi^2 T^2), \\ h_1 &= H^2(\mu)/(2\pi^2) & h'_1 &= -H^0(\mu)/(4\pi^2 T^2), \end{aligned}$$

$$h = 3h_0[h_0 + \mu^2 h_1] \quad h' = 3h'_0[h_0 + \mu^2 h_1] + 3h_0[h'_0 + h_1/T^2 + \mu^2 h'_1] \quad (6)$$

with $\mu = M_\pi/T$. Also $b_{eff} = b - \frac{0.6T}{\pi^3 F^4 M_\pi}$, $b'_{eff} = -\frac{1}{\pi^3 F^4 M_\pi^2} \left(\frac{5}{16} - \frac{0.3T}{M_\pi} \right)$ and $a' = \frac{2a}{m_\pi^2} + \frac{3}{32\pi F^2} \left(1 - \frac{35m_\pi^2}{32\pi^2 F^2} \right)$. The constant $c \simeq 0.9$ and $F_\pi/F = 1.057 \pm 0.012$ with $F_\pi = 93 MeV$ [13]. The constants a and b are related to the S-wave and D-wave π - π scattering lengths respectively [13]. Finally the functions $H^n(\mu)$ are given as [14]

$$H^n(\mu) = \int_0^\infty \frac{x^n dx}{\sqrt{x^2 + \mu^2}} \frac{1}{e^{\sqrt{x^2 + \mu^2}} - 1}. \quad (7)$$

We have extracted the temperature dependence of the condensate as in Eq.(5) for low temperatures. For temperatures close to T_c , the critical behaviour is that of O(4) spin model in three dimension [15] and has also been seen in lattice QCD simulations [16]. The order parameter here is given as $\frac{\langle \bar{q}q \rangle_T}{\langle \bar{q}q \rangle_{T=0}} = \left(1 - \frac{T}{T_c} \right)^\beta$, where $\beta = 0.39$ [7]. We have taken $T_c = 150 MeV$ [7]. The two regions are joined smoothly and the result is shown in Fig. 1(a). This result is fitted with Eq. (4) to determine $S(T) = R(0)/R(T)$, which is plotted in Fig. 1(b). We shall use it to calculate the quark propagator and the hadronic correlation functions.

III. QUARK PROPAGATION IN THERMAL VACUUM

In the calculation of correlators, quark propagators enter in a direct manner and hence it is instructive to study aspects of the interacting propagator in some detail [6].

The equal time interacting quark Feynman propagator in the condensate vacuum is given as $S_{\alpha\beta}(\vec{x}) = \left\langle \frac{1}{2} \left[\psi_\alpha^i(\vec{x}), \bar{\psi}_\beta^i(0) \right] \right\rangle$, which at finite temperature reduces to

$$S(\vec{x}, T) = \frac{1}{2} \frac{\delta^{ij}}{(2\pi)^3} \int e^{i\vec{k}\cdot\vec{x}} \cos 2\theta [\sin 2h - \vec{\gamma} \cdot \hat{k} \cos 2h] d\vec{k}. \quad (8)$$

$$= \frac{i}{4\pi^2} \frac{\vec{\gamma} \cdot \vec{x}}{x^2} [I_1(x) - I_2(x)] + \frac{1}{4\pi^2} \frac{I_3(x)}{x} \quad (9)$$

where,

$$I_1(x) = \int_0^\infty k \left(\cos kx - \frac{\sin kx}{kx} \right) \cos 2\theta dk, \quad (10)$$

$$I_3(x) = \int_0^\infty k \sin kx \cos 2\theta e^{-R^2(T)k^2} dk, \quad (11)$$

$$I_2(x) = \int_0^\infty k \left(\cos kx - \frac{\sin kx}{kx} \right) \cos 2\theta \frac{e^{-R^2(T)k^2}}{1 + (1 - e^{-R^2(T)k^2})^{1/2}} dk, \quad (12)$$

with $x = |\vec{x}|$, $k = |\vec{k}|$.

The free massive propagator, which can be derived from $S(\vec{x}, T)$ by the substitutions $\sin 2f(k) = m_q/\epsilon$ and $\cos 2f(k) = k/\epsilon$, is given as

$$S_0(m_q, \vec{x}, T) = \frac{1}{(2\pi)^2} \frac{1}{x} \left[m_q (m_q K_1(m_q x) - 2I_5(x)) - i \frac{\vec{\gamma} \cdot \vec{x}}{x} (m_q^2 K_2(m_q x) + 2I_6(x)) \right] \quad (13)$$

$$\text{where } I_5(x) = \int_0^\infty \frac{k}{\epsilon} \sin(kx) \sin^2 \theta dk, \quad I_6(x) = \int_0^\infty \frac{k^2}{\epsilon} \left(\cos kx - \frac{\sin kx}{kx} \right) \sin^2 \theta dk.$$

$K_1(m_q x)$ and $K_2(m_q x)$ are the first and second order modified Bessel functions of the second kind respectively.

In Fig. 2 we plot the two components $\text{Tr } S(\vec{x}, T)$ and $\text{Tr } (\gamma \cdot \hat{x}) S(\vec{x}, T)$ of the propagator for massless interacting quarks given by Eq. (9) at $T = 0$ MeV, $T = 100$ MeV and $T = 135$ MeV, corresponding to the chirality flip and non-flip components considered by Shuryak and Verbaarschot [17]. The normalisation is discussed in our earlier work [6]

To compare with the constituent quark models with an effective constituent mass, we have also plotted the behaviour of free massive quark propagator with masses 100 MeV, 200 MeV and 300 MeV. In the chirality flip part, the propagator in the condensate medium starts from zero, consistent with zero quark mass at small distances, attains a maximum value of about 250 MeV at a distance of about 0.9 fm and then falls off gradually. Further the interacting propagator overshoots the massive propagators after about 0.6 fm. We also see that with increasing temperature, the chirality flip component has a lower peak and the position of the peak shifts towards higher distances indicating the decrease of the dynamical mass with temperature.

In the chirality non flip part, the interacting propagator starts from 1, again consistent with the behaviour expected from asymptotic freedom. But at larger separation it falls rather fast indicative of an effective mass of the order of 150 MeV. These features are qualitatively

similar to that of the quark propagator at zero temperature [6,17], though quantitatively there are differences. Also, the non-flip component falls faster with increase of temperature.

Clearly therefore, similar to the situation at zero temperature, whereas a constituent quark description is adequate to describe the behaviour of the chirality nonflip part of the propagator, it is not so for the chirality flip part.

IV. MESON CORRELATION FUNCTIONS

In our earlier work, we noted that phenomenology of correlation functions necessitated introduction of irreducible four point structure (or fluctuations of the condensate fields) in vacuum [11]. In fact, the meson correlation functions were different from square of the two point function (propagator) and the difference could be expressed in terms of the four point function. The expression of the meson correlation function at zero temperature defined in our earlier work [11] can be extended to finite temperatures as,

$$R(\vec{x}, T) = Tr \left[S(\vec{x}, T) \Gamma' S(-\vec{x}, T) \Gamma \right] + Tr \langle | \left[\Sigma(\vec{x}) \Gamma' \Sigma(-\vec{x}) \Gamma \right] | \rangle_T \quad (14)$$

Where $J(x) = \bar{\psi}_\alpha^i(x) \Gamma_{\alpha\beta} \psi_\beta^j(x)$, is a generic meson current with Γ being a 4×4 matrix ($1, \gamma_5, \gamma_\mu$ or $\gamma_\mu \gamma_5$), x is a four vector; α and β are spinor indices; i and j are flavour indices. The field $\Sigma(\vec{x})$ is the condensate fluctuation field introduced in Ref. [11] to include four point irreducible structures in QCD vacuum..

Thus, at finite temperature the correlator (Eq. 14) is now the square of the interacting equal time *thermal* propagator plus the four point contribution at finite temperature. The thermal quark propagator was obtained in the earlier section. We keep the structure of the fields $\Sigma(x, T)$ the same as for zero temperature [11].

$$\Sigma_{\alpha\beta}(\vec{x}) = \Sigma_{\alpha\beta}^V(\vec{x}) + \Sigma_{\alpha\beta}^S(\vec{x}) \quad (15)$$

$$= \mu_1^2 (\gamma^i \gamma^j)_{\alpha\beta} \epsilon_{ijk} \phi^k(\vec{x}) + \mu_2^2 \delta_{\alpha\beta} \phi(\vec{x}) \quad (16)$$

where the first term corresponds to vector fluctuations and the second to scalar. μ_1 and μ_2 in the above equations are dimensional parameters which give the strength of the fluctuations

and $\phi^k(\vec{x})$ and $\phi(\vec{x})$ are vector and scalar fields such that, with $|\Omega\rangle$ as the ground state of QCD, we have

$$\langle\Omega|\phi^i(\vec{x})\phi^j(0)|\Omega\rangle = \delta^{ij}g_V(\vec{x}); \quad \langle\Omega|\phi(\vec{x})\phi(0)|\Omega\rangle = g_S(\vec{x}) \quad (17)$$

At finite temperature, the functions g_V and g_S will be temperature dependent. We do not know how to calculate it except for a general property that the effect of the four point structure should decrease with temperature. We take here a simple ansatz for the temperature dependence of g_V and g_S ,

$$g_{S,V}(x, T) = \left(\frac{\langle\bar{q}q\rangle_T}{\langle\bar{q}q\rangle_{T=0}} \right)^2 g_{S,V}(x, T=0) \quad (18)$$

Similar to calculations at zero temperature, we shall consider the ratio of the physical correlation function to that of massless noninteracting quarks at zero temperature given as

$$R_0(x) = Tr [S_0(x)\Gamma' S_0(-x)\Gamma]$$

. The normalised correlation functions thus defined as

$$C(\vec{x}, T) = \frac{R(\vec{x}, T)}{R_0(\vec{x})} \quad (19)$$

are plotted in Figure 3 for the pseudoscalar and vector channels.

As expected (on physical grounds) the amplitude of the correlator decreases with increasing temperature. The peak of the vector correlator shifts towards the right after $T = 0.9T_c$. We might remind ourselves that the position of the peak of the correlator is inversely proportional to the mass of the particle in the relevant channel [4].

The spatial hadronic correlators have been used to extract the hadronic screening masses and widths at finite temperature [9]. To extract the hadronic properties at finite temperature, we use a phenomenological parameterisation as is usually done in sum rule calculations [18,19]. We may note here however, that the phenomenological inputs are not available at finite temperature. The correlators are parameterised with the mass, decay width and the coupling of the particle to the vacuum, all three parameters being temperature dependent. We first express the correlator in terms of spectral density function.

$$R_{ph}(\vec{x}) = \int_0^\infty ds \frac{\sqrt{s}}{4\pi^2 x} K_1(\sqrt{s}x) \rho(s) \quad (20)$$

Then we use the following phenomenological parameterisation for the spectral density function [18,19],

$$\rho^V(s) = 3\lambda_\rho^2 \delta(s - M_\rho^2) + \frac{3s}{4\pi^2} \tanh\left[\frac{\sqrt{s}}{4T}\right] \theta(s - s_o) + T^2 S_\rho \delta(s) \quad (21)$$

$$\rho^P(s) = \lambda_\pi^2 \delta(s - M_\pi^2) + \frac{3s}{8\pi^2} \tanh\left[\frac{\sqrt{s}}{4T}\right] \theta(s - s_o) \quad (22)$$

where λ is the coupling of the bound state to the current, M is mass of the bound state and s_o is the threshold for continuum contributions. The last term in Eq. (21) is the scattering term for soft thermal dissociations (mainly through pions), which exists only at finite temperature [18]. This term is given as

$$S_\rho = \lim_{|\vec{p}| \rightarrow 0} \frac{1}{2\pi} \int_0^{|\vec{p}|^2} d\omega^2 \int_v^\infty x^2 \left(n\left(\frac{|\vec{p}|x - \omega}{2T}\right) - n\left(\frac{|\vec{p}|x + \omega}{2T}\right) \right) \quad (23)$$

The derivation of the above expression is slightly tricky and we have given it in the appendix. Following Ref. [18] we take $S_\rho \approx \frac{T^2}{9}$.

The mass, threshold and coupling are then extracted such that the correlators as obtained from Eq. 20 agree with the normalised correlation functions as calculated by us (Fig. 3) [11]. This is done for each temperature. The results are plotted in Fig. 4 for the pseudoscalar channel and in Fig. 5 for the vector channel. The results are also shown in Table I.

V. SUMMARY AND CONCLUSIONS

As can be seen from Fig. 3, with increase in temperature, the correlation functions have a lower peak indicating lack of correlations with temperature. In the vector channel the mass of the ρ meson appears to decrease beyond 120 MeV. The threshold for the continuum also decreases around the same temperature. The behaviour with temperature of these quantities is qualitatively similar to that found by Hatsuda *et al* [19]. We have also plotted

the temperature dependence of the coupling of the boundstate to the current which decreases with temperature but rather slowly as compared to mass or the threshold for the continuum. The temperature dependence of these parameters can be used to calculate the lepton pair production rate from ρ in the context of ultra relativistic heavy ion collision experiments to estimate vector meson mass shift in the medium.

In the pseudoscalar channel the mass remains almost constant till the critical temperature whereas the threshold and the coupling decrease with the temperature [20]. We may note here that in the pseudoscalar channel, the contribution to the correlation function mostly comes from the fluctuating fields and the temperature behaviour as taken in Eq.(18) essentially does not shift the position of the peak whereas the magnitude of the correlator decreases. That is reflected in the above behaviour of the parameters in the pseudoscalar channel. We may note here that similar behaviour of pion mass becoming almost insensitive to temperature below the critical temperature was also observed in Ref. [20] where correlation functions were calculated in a QCD motivated effective theory namely the Nambu- Jona Lasinio model.

We would like to add here that the present analysis will be valid for temperatures below the critical temperature. Above the critical temperature there have been calculations essentially using finite temperature perturbative QCD in random phase approximations [21]. However, in the region above T_C , nonperturbative features have been seen to exist from studies in lattice QCD simulations [7]. In view of this, one possibly has to do a hard thermal loop calculation where a partial resummation is done [22].

VI. ACKNOWLEDGEMENT

The present work was initiated when one of the authors (HM) was visiting Department of Physics, University of Bielefeld. He would like to thank the Physics Department there for providing the facilities and Alexander von Humboldt Foundation, Germany for a fellowship during that period.

APPENDIX A:

Here we shall derive the scattering term S_ρ . This may be calculated by considering the imaginary part of the longitudinal correlator for space like four momenta and can be written as

$$\rho_l^s(\omega, \vec{p}) = \frac{Im \Pi_{00}}{|\vec{p}^2|} \quad (\text{A1})$$

which is explicitly written as [24]

$$\rho_l^s(\omega, \vec{p}) = 2 \times \frac{(2\pi)^4}{|\vec{p}^2|} \int \frac{d^3 k_1}{2E_1(2\pi)^3} \frac{d^3 k_2}{2E_2(2\pi)^3} |\langle \pi(\vec{k}_1) | J_0 | \pi(\vec{k}_2) \rangle|^2 \quad (\text{A2})$$

$$\times \delta(\omega - E_1 + E_2) \delta^{(3)}(\vec{p} - k_1 + k_2) (n_2 - n_1). \quad (\text{A3})$$

Here $E_1 = \sqrt{\vec{k}_1^2 + m_\pi^2}$; $E_2 = \sqrt{\vec{k}_2^2 + m_\pi^2}$ and $n_i \equiv n(E_i)$ is the Bose distribution function for pions.

In general the expectation of a vector current with respect to a pion state is given as [23]

$$\langle \pi(k_1) | J_\mu | \pi(k_2) \rangle = (k_1 + k_2)_\mu G_\pi(p) \quad (\text{A4})$$

where, $p = k_1 - k_2$ and $G_\pi(p)$ is the pion form factor with $G_\pi(0) = 1$ Substituting this in Eq. (A3) and integrating over k_2 we obtain

$$S_\rho(\omega, \vec{p}) = 2 \times \frac{2}{(2\pi)^2} 4|\vec{p}^2| \int \frac{d^3 k_1}{E_1} (G_\pi(p))^2 \delta(\omega - E_1 + E - 2)(2E_1 - \omega)^2 (n_2 - n_1) \quad (\text{A5})$$

with $\vec{k}_2 = \vec{p} - \vec{k}_1$. Next, since the delta function above contribute to space like ($p^2 < 0$) region we write it as

$$\delta(\omega - E_1 + E_2) = 2E_2 \delta((\omega - E_1)^2 - E_2^2) \theta(-p^2)$$

To simplify further, we may change the integration over three momentum \vec{k}_1 to the integration over energy E_1 and the angle $\cos \theta_{\vec{p}, \vec{k}}$. Performing the integration over angles restricts the lower limit of the energy integral E_1 as $E_{1min} = \frac{1}{2}(\omega + |\vec{p}|v)$, where, $v = (1 - \frac{4m_\pi^2}{p^2})^{1/2}$.

Thus we have

$$\rho_l^s(\omega, \vec{p}) = \frac{1}{4\pi} |\vec{p}|^3 \int_{E_{min}}^{\infty} G_\pi^2(p) (2E_1 - \omega)^2 (n_2 - n_1) \quad (\text{A6})$$

with $E_2 - E_1 - \omega$. Next, defining the variable x through $E_1 = \frac{1}{2}(\omega + |\vec{p}|x)^{1/2}$, leads to

$$\rho_l^s(\omega, \vec{p}) = \frac{1}{8\pi} \int_v^{\infty} dx x^2 n\left(\frac{|\vec{p}|x - \omega}{2T}\right) G_\pi^2(p) (2E_1 - \omega)^2 (n_2 - n_1) \quad (\text{A7})$$

We shall consider the longitudinal form factor $S_\rho(\omega, \vec{p})$ in a frame which is at rest with respect to the medium which implies that $\vec{p} \rightarrow 0$. In this limit the constraint $0 < \omega < \vec{p}^2$ also forces ω to approach zero. However the above integral becomes increasingly large as $\vec{p} \rightarrow 0$ such that the integrated quantity of $S_\rho(\omega, \vec{p})$ within the phase space for ω remains finite. Thus we first integrate over this region with \vec{p} finite and then take the limit $\vec{p} \rightarrow 0$. Thus let

$$I = \lim_{|\vec{p}| \rightarrow 0} \int_0^{|\vec{p}|^2} d\omega^2 \rho_l^s(\omega, \vec{p}) = \frac{S_\rho}{2\pi} \quad (\text{A8})$$

so that $\rho_l^s(\omega, \vec{p})$ effectively becomes a delta function. Thus the spectral density reduces to

$$\lim_{|\vec{p}| \rightarrow 0} \rho_l^s(\omega, \vec{p}) = \delta(\omega^2) \frac{S_\rho}{2\pi} \quad (\text{A9})$$

We also note that there arises no ambiguity from the pion form factor as $G_\pi(p=0) = 1$.

Now the integral I can be written as

$$I = \frac{1}{8\pi} \lim_{|\vec{p}| \rightarrow 0} \int_0^{|\vec{p}|^2} d\omega^2 \int_v^{\infty} dx x^2 [n((|\vec{p}|x - \omega)/2T) - n((|\vec{p}|x + \omega)/2T)] \quad (\text{A10})$$

We change the integration variables [25] by putting $\omega = |\vec{p}|\lambda$ and $x = \sqrt{1 + \frac{y^2}{|\vec{p}|^2(1-\lambda^2)}}$. Hence the spectral density function can be written as

$$I = \frac{1}{4\pi} \lim_{|\vec{p}| \rightarrow 0} \int_0^1 d\lambda \lambda \int_{2m_\pi}^{\infty} \frac{xy dy}{(1-\lambda^2)^2} \left[n\left(\frac{|\vec{p}|x - \omega}{2T}\right) - n\left(\frac{|\vec{p}|x + \omega}{2T}\right) \right] \quad (\text{A11})$$

In the limit of $|\vec{p}| \rightarrow 0$, we may Taylor expand the difference of the distribution functions in the square bracket of eq.(A11) and have

$$\left[n\left(\frac{|\vec{p}|x - \omega}{2T}\right) - n\left(\frac{|\vec{p}|x + \omega}{2T}\right) \right] \approx -\frac{2x|\vec{p}|^2(1-\lambda^2)^2}{y^2} \frac{dn}{d\lambda}.$$

Substituting back in eq. (A11) and performing an integration by parts for $d\lambda$ integration we have

$$I = \frac{1}{2\pi} \int_0^1 d\lambda \int_{2m_\pi}^\infty dy n\left(\frac{y}{2T\sqrt{1-\lambda^2}}\right) y. \quad (\text{A12})$$

In the limit of vanishing pion mass we have $I = 2\pi T^2/9$ so that $S_\rho = T^2/9$.

REFERENCES

- [1] E.V. Shuryak, *The QCD vacuum, hadrons and the superdense matter* (World Scientific, Singapore, 1988).
- [2] M.A. Shifman, A.I. Vainshtein and V.I. Zakharov, Nucl.Phys. B147, 385, 448 and 519(1979).
- [3] E.V. Shuryak, Rev. Mod. Phys. 65, 1 (1993).
- [4] M.-C. Chu, J.M. Grandy, S. Huang and J.W. Negele, Phys. Rev. D48, 3340 (1993) ;
ibid, Phys. Rev. D49 6039(1994).
- [5] A. Mishra, H. Mishra, S.P. Misra, P.K. Panda and Varun Sheel, Int. J. Mod. Phys. E5,
93 (1996).
- [6] Varun Sheel, Hiranmaya Mishra and Jitendra C. Parikh, Int. J. Mod. Phys. E6, 275,
(1997).
- [7] E. Laermann, Nucl. Phys. A610, 1c (1996).
- [8] E.V. Shuryak, Nucl. Phys. A544, 65c (1992).
- [9] T. Schäfer and E.V. Shuryak, Phys. Rev. D54, 1099 (1996)
- [10] T. Hatsuda, Y. Koike and S.H. Lee, Nucl. Phys. B394, 221 (1993);
- [11] Varun Sheel, Hiranmaya Mishra and Jitendra C. Parikh, Phys. Lett. B382, 173 (1996).
- [12] H. Umezawa, H. Matsumoto and M. Tachiki *Thermofield dynamics and condensed states*
(North Holland, Amsterdam, 1982) ; P.A. Henning, Phys. Rep.253, 235 (1995).
- [13] P. Gerber and H. Leutwyler, Nucl. Phys. B321, 387 (1989).
- [14] H.-S. Roh and T. Matsui, nucl-th/9611050
- [15] K. Rajgopal and F. Wilczek, Nucl. Phys. B399, 395 (1993).

- [16] F. Karsch, Phys. Rev. D49, 3791 (1994). ; F. Karsch and E. Laermann, Phys. Rev. D50, 6954 (1994).
- [17] E.V. Shuryak and J.J.M. Verbaarschot, Nucl. Phys. B410, 37 (1993).
- [18] C. Adami, T. Hatsuda and I. Zahed, Phys. Rev. D43, 921 (1991) .
- [19] Tetsuo Hatsuda, Yuji Koike and Su Hounq Lee, Nucl. Phys. B394, 221 (1993).
- [20] T. Hatsuda and T. Kunihiro, Prog. Theor. Phys. Suppl. 91, 284 (1987).
- [21] Jitendra C. Parikh, Philip J. Siemens, Phys. Rev. D37, 3246 (1988); R.B. Thayyullathil and J.C. Parikh, Phys. Rev. D44, 3964, (1991).
- [22] Eric Braaten and Robert D. Pisarski, Phys. rev. Lett. 64, 1338 (1990), Nucl. Phys. B339, 310 (1990).
- [23] J.F. Donoghue, E. Golowich and B.R. Holostein, *Dynamics of the standard model*, (Cambridge university press, 1992).
- [24] A. A. Abrikosov, L. P. Gorkov and I. E. Dzyaloshinski, *Methods of Quantum Field Theory in Statistical Physics*, (Prentice-Hall, Engelwood Cliffs, N. J., 1963)
- [25] S. Mallik and K. Mukherjee, hep-ph/9711297

FIGURES

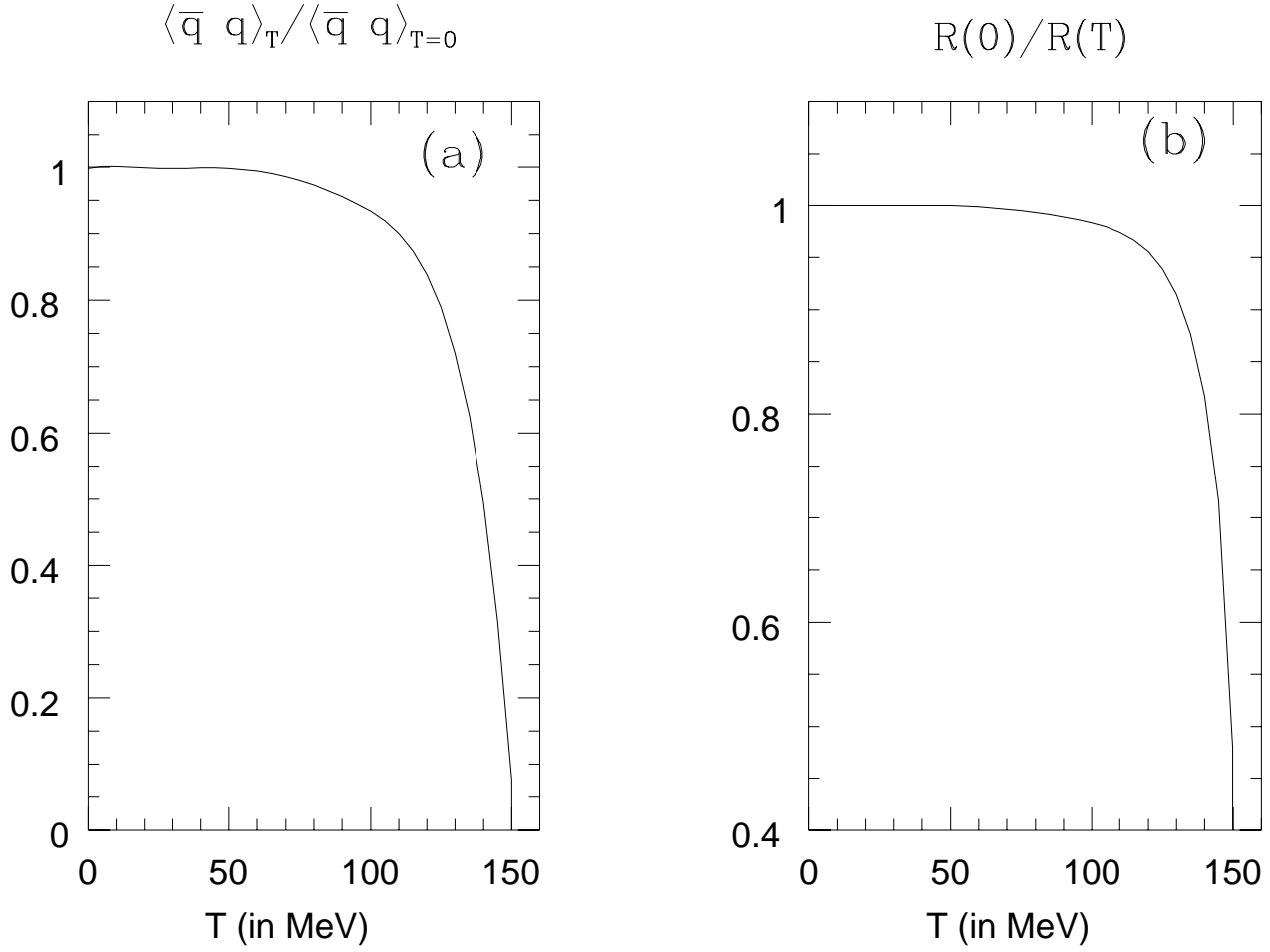


FIG. 1. Figure (a) shows quark condensate at finite temperature normalised to that at zero temperature obtained from CHPT and Lattice. Figure (b) shows $R(0)/R(T)$ as determined from Fig (a).

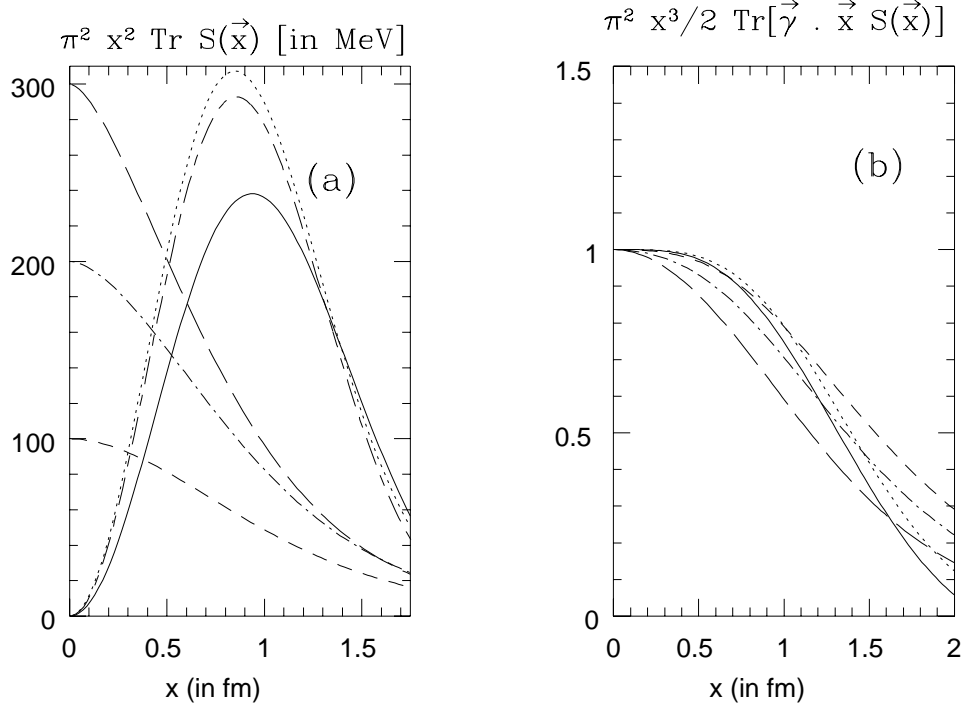


FIG. 2. The two components of the thermal quark propagator, (a) $\text{Tr}(S)$ and (b) $\text{Tr}[(\vec{\gamma} \cdot \hat{x})S]$ versus the distance x (in fm). The three lines, dot, short dash-long dash and solid corresponds to massless quark interacting propagator $S(x, T)$ at temperatures of 0, 100 and 135 MeV respectively. The three lines, short dashed, dot-short dashed and long dashed correspond to a massive free propagator with a mass of 100, 200 and 300 MeV, respectively at $T=135$ MeV.

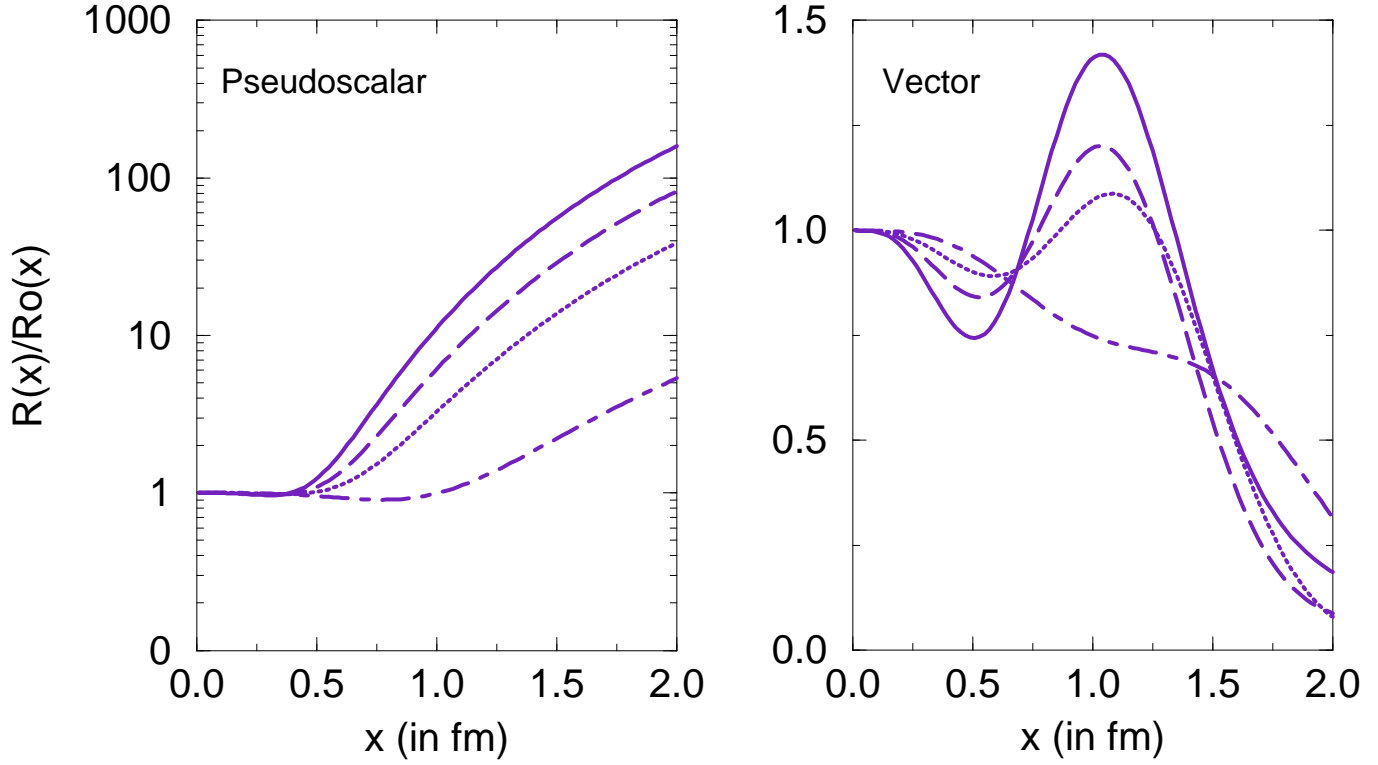


FIG. 3. The ratio of the meson correlation functions at finite temperature to the correlation functions for noninteracting massless quarks at zero temperature $\frac{R(x,T)}{R_0(x,T=0)}$, vs. distance x (in fm). The solid, dashed, dotted and dot-dashed lines correspond to temperatures $T = 0$ MeV, $T = 130$ MeV, $T = 140$ MeV and $T = 148$ MeV respectively.

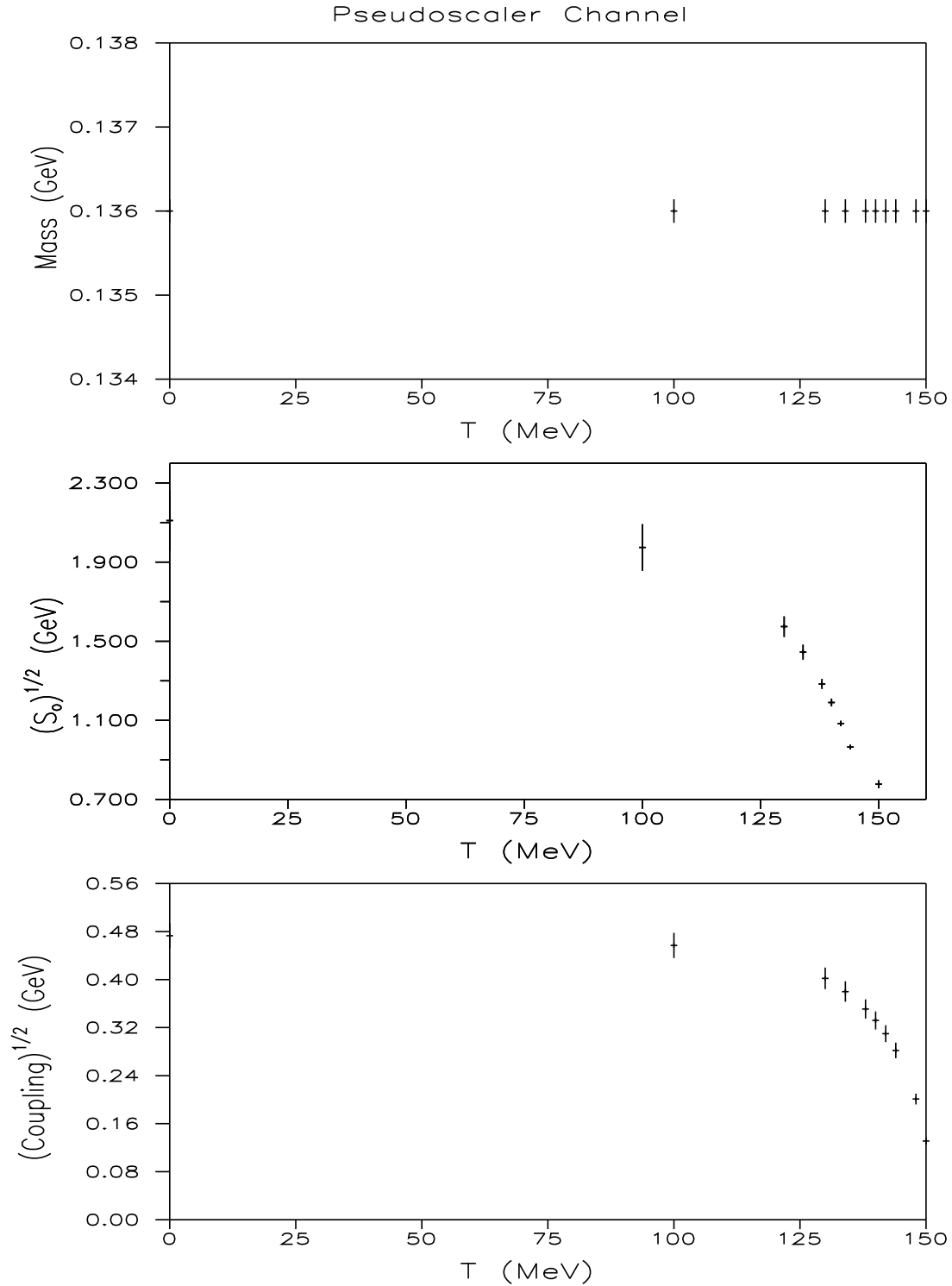


FIG. 4. The temperature dependence of mass, threshold (S_0) and coupling for the pseudoscalar channel. $T_c = 150$ MeV. The vertical lines represent the errors obtained while fitting

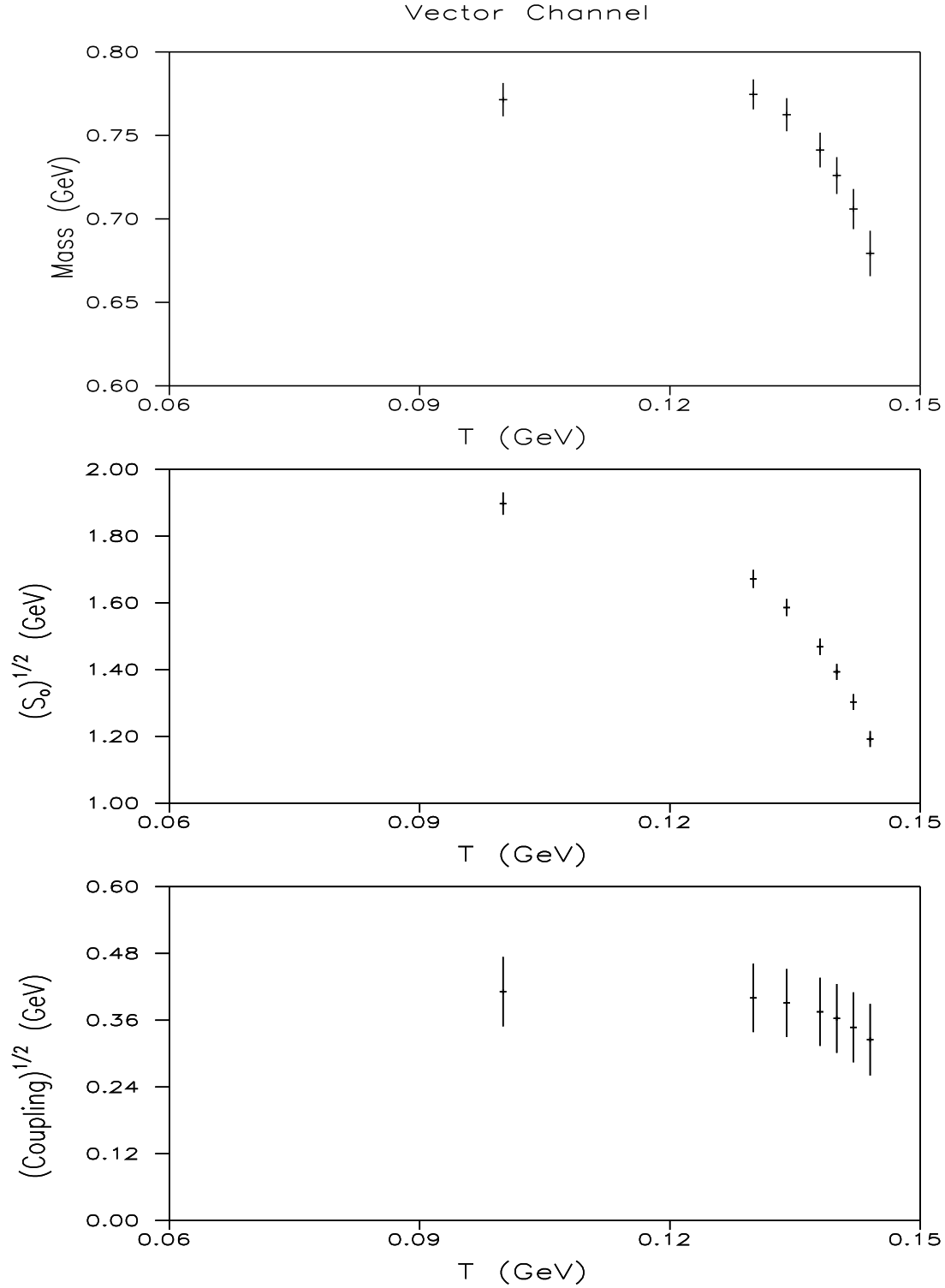


FIG. 5. The temperature dependence of mass, threshold (S_0) and coupling for the vector channel. $T_c = 150$ MeV. The vertical lines represent the errors obtained while fitting

TABLES

TABLE I. Fitted parameters

CHANNEL	Temp.(MeV)	M (GeV)	λ	$\sqrt{s_0}$ (GeV)
Vector	0	0.780 ± 0.005	$(0.420 \pm 0.041 \text{ GeV})^2$	2.070 ± 0.035
	100	0.771 ± 0.001	$(0.411 \pm 0.062 \text{ GeV})^2$	1.897 ± 0.033
	130	0.774 ± 0.001	$(0.402 \pm 0.061 \text{ GeV})^2$	1.672 ± 0.027
	134	0.762 ± 0.001	$(0.391 \pm 0.061 \text{ GeV})^2$	1.586 ± 0.026
	138	0.741 ± 0.001	$(0.375 \pm 0.061 \text{ GeV})^2$	1.468 ± 0.024
	140	0.726 ± 0.001	$(0.363 \pm 0.062 \text{ GeV})^2$	1.393 ± 0.024
	142	0.706 ± 0.001	$(0.347 \pm 0.063 \text{ GeV})^2$	1.303 ± 0.024
	144	0.679 ± 0.001	$(0.325 \pm 0.064 \text{ GeV})^2$	1.192 ± 0.024
Pseudoscalar	0	0.136 ± 0.00014	$(0.473 \pm 0.021 \text{ GeV})^2$	2.110 ± 0.152
	100	0.136 ± 0.00014	$(0.457 \pm 0.021 \text{ GeV})^2$	1.974 ± 0.118
	130	0.136 ± 0.00014	$(0.402 \pm 0.018 \text{ GeV})^2$	1.574 ± 0.052
	134	0.136 ± 0.00014	$(0.380 \pm 0.017 \text{ GeV})^2$	1.445 ± 0.038
	138	0.136 ± 0.00014	$(0.351 \pm 0.016 \text{ GeV})^2$	1.284 ± 0.025
	140	0.136 ± 0.00014	$(0.332 \pm 0.015 \text{ GeV})^2$	1.190 ± 0.020
	142	0.136 ± 0.00014	$(0.310 \pm 0.014 \text{ GeV})^2$	1.084 ± 0.014
	144	0.136 ± 0.00014	$(0.282 \pm 0.013 \text{ GeV})^2$	0.965 ± 0.011
	148	0.136 ± 0.00014	$(0.201 \pm 0.009 \text{ GeV})^2$	0.970 ± 0.020
	150	0.136 ± 0.00014	$(0.131 \pm 0.006 \text{ GeV})^2$	0.777 ± 0.020